Vision Res. Vol. 30, No. 4, pp. 515–525, 1990
Printed in Great Britain.

0042-6989/90 $3.00 + 0.00

EVALUATION OF PUPIL CONSTRICTION AND DILATION FROM CYCLING MEASUREMENTS

JOHN G. MILTON* and ANDRÉ LONGTIN†
Departments of Physiology and Physics, McGill University, Montreal, Quebec, Canada H3G 7Y6

(*Received* 1 *November* 1988; *in revised form* 12 *June* 1989)

Abstract—Pupil cycling was produced using an electronic circuit so that the retina was illuminated in Maxwellian view only when pupil area exceeded an adjustable area threshold, A_{ref}. The maximum (A_{max}) and minimum (A_{min}) amplitude of the oscillations varied linearly with A_{ref}. These observations are described by a delay–differential equation. The A_{ref}-dependent changes in A_{max}, A_{min} were used, respectively, to quantitate dilation and constriction. A comparison of the predicted and observed period of pupil cycling suggests that the latency times for light onset and offset are the same. Measurements of A_{max}, A_{min} provide a method for determining the average pupil light response.

Pupil light reflex Pupil constriction Pupil dilation Delay-differential equations

INTRODUCTION

Pupil constriction and dilation are typically evaluated from the changes in pupil area following a single light pulse. The accuracy of this method is limited by the effects of pupillary hippus and the intrinsic variability in the response of the pupil to identical light pulses (Usui & Stark, 1982). Consequently, quantitative characterization of the pupil light response requires that a large number of pupil responses to individual light pulses be averaged (see, for example, Semmlow & Chen, 1977; Sun, Tauchi & Stark, 1983a; Usui & Stark, 1982).

An alternative method for evaluating pupil movements involves inducing regular oscillations in pupil area ("pupil cycling") by either using a slit lamp to focus a narrow light beam at the pupillary margin (Stern, 1944; Miller & Thompson, 1978) or by combining an infrared video-pupillometer with an electronic circuit which regulates retinal light flux as a function of pupil area (Stark, 1962; Longtin & Milton, 1988; Milton, Longtin, Kirkham and Francis, 1988; Reulen, Marcus, van Gilst, Koops, Bos, Tiesinga, de Vries & Boshuizen, 1988). Measurements of pupil cycling are important as a clinical test for detecting pathology within the pupil light reflex pathways. For example, a prolongation of the period of pupil cycling has been reported for a variety of afferent (Miller & Thompson, 1978) and efferent (Martyn & Ewing, 1986) pupillary defects, whereas an intermittent irregularity in pupil cycling occurs in demyelinative optic neuropathies (Ukai et al., 1980; Milton et al., 1988).

Here we show that measurements of the amplitude of pupil area oscillations reflect properties of the efferent arc of the pupil light reflex. This observation permits the development of a method for evaluating pupil movements from cycling measurements which offers a number of advantages over methods based on the pupil's response to single light pulses.

METHODS

Subjects were healthy males and females ($n = 5$; ages 20–45 years) who were free from both ocular disease and disorders known to affect autonomic function. The experimental conditions and design of our experiment are the same as described previously (Longtin & Milton, 1988; Milton et al., 1988). A narrow light beam (diameter 1.2 mm; retinal illumination was 375–750 td; peak wavelength 605 nm) was focussed on the center of the pupil ('Maxwellian view') to "open" the feedback loop present in the pupil light reflex (Stark & Sherman, 1957). When subjects were adapted for at least 15 min in a room lit only by a dim red light, the smallest pupil diameter was

*To whom correspondence should be addressed at: Department of Neurology, Box 425, University of Chicago Hospitals, 5841 South Maryland Avenue, Chicago, IL 60637, U.S.A.
†Present address: Theoretical Division B213, Los Alamos National Laboratory, Los Alamos, NM 87545, U.S.A.

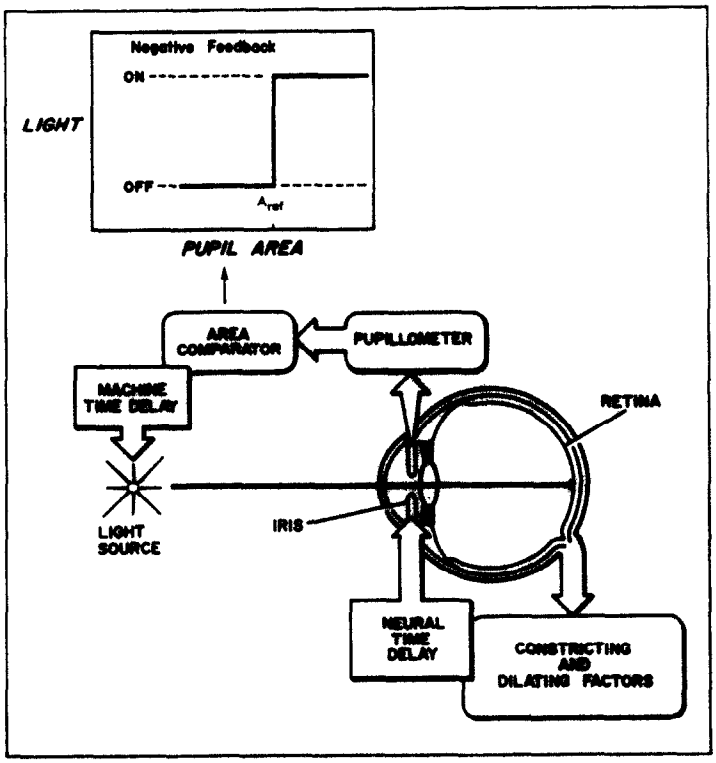

Fig. 1. Schematic representation of the pupil light reflex with imposed external feedback. The area comparator used for pupil cycling compared the pupil area, A, to an adjustable area threshold, A_{ref}: when $A > A_{ref}$ the light was turned on and illuminated the retina in Maxwellian view, otherwise it was off. This area comparator corresponds to negative feedback since the pupil constricts when $A > A_{ref}$ (the light is on). It is piecewise constant negative feedback since the illumination can take on only one of two values, i.e. on or off.

~4–5 mm. We used the measured pupil area to control the timing and duration of the light pulses falling on the retina by modifying the technique of environmental 'clamping' suggested by Stark (1962) (Fig. 1). This was accomplished by comparing the analog output of an infrared video-pupillometer (Hamamatsu Iriscorder C-2515) to an adjustable area threshold, A_{ref}, by using an electronic circuit (area comparator in Fig. 1). The area comparator was constructed using standard voltage comparators (LM392H), operational amplifiers (LM741) and logic gates (74LS00) and was designed to simulate piecewise constant negative feedback (see legend to Fig. 1). The retinal light intensity can take on only one of two values depending on whether the pupil area is greater than or less than A_{ref}. This area comparator is an idealization of the method of edge-light pupil cycling, where A_{ref} corresponds to the pupil area at which the positions of the slit lamp beam and the pupillary margin coincide. However, in our method the illumination is not at the pupillary margin, but is in Maxwellian view. The advantages of the electronic method of pupil cycling over that of edge-light pupil cycling are (Milton et al., 1988): (1) the pupil area oscillations are easier to obtain and control experimentally; and (2) the oscillations can be studied over a range of pupil areas by varying A_{ref} (Fig. 2).

The pupil images were analyzed by a frame grabber that counts the number of pixels above a gray level set by the experimenter to discriminate between pupil and iris. The sampling rate of the pupillometer was 60 Hz and the linearity is better than 1% from 0 to 150 mm^2 with an accuracy of 0.01 mm^2. The bandwidth of the pupillometer is well beyond that of the pupil light reflex [about 5 Hz: Stark (1959)]. Hence, for all practical purposes, the response time of the pupillometer can be neglected on the time scale of the phenomena we are considering in this study. However, the following image and signal processing (~25 msec) and triggering of the light pulse (~75 msec) add a 100 msec pure delay ("machine delay") to the normal physiological delay of this reflex (~300 msec for the retinal illuminance used in this study (Milton et al., 1988). The pupil latency time (delay) following light onset was evaluated as the time

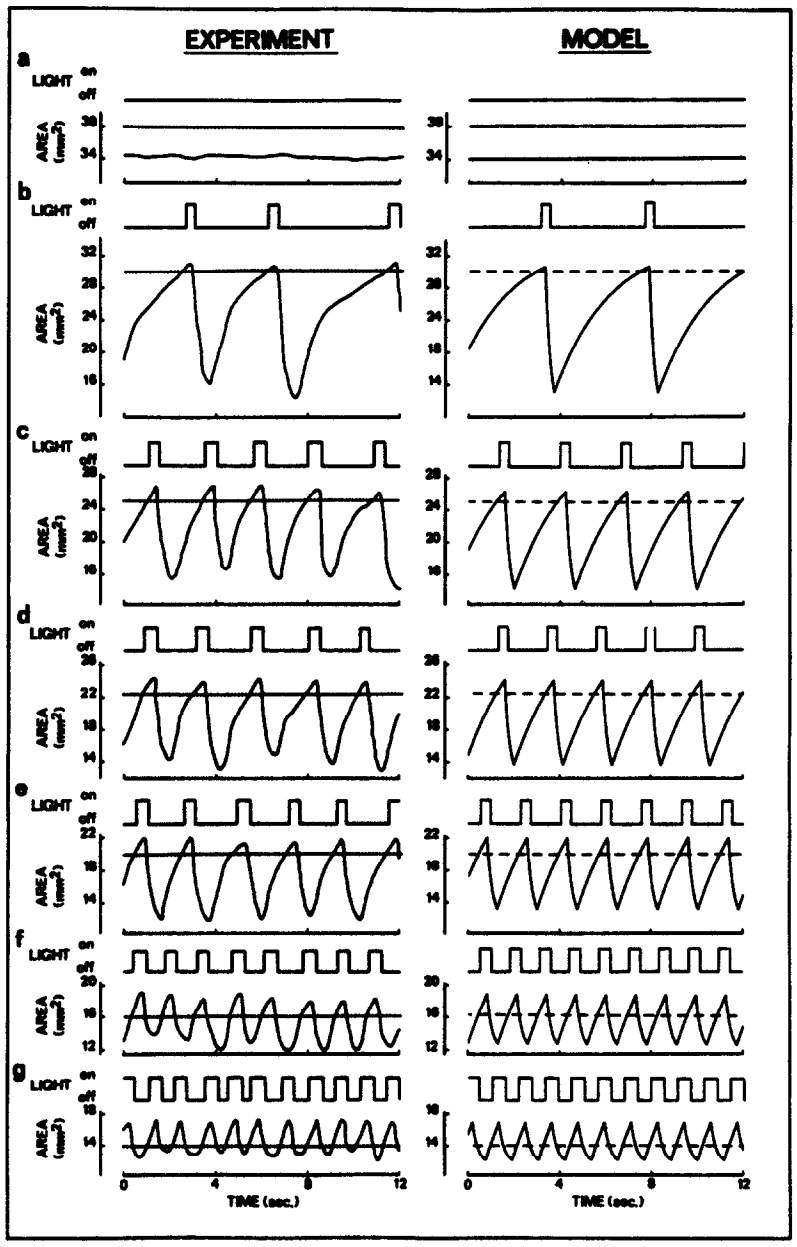

Fig. 2. Pupil cycling with imposed piecewise constant negative feedback (Fig. 1) as a function of A_{ref} for subject A in Table 2 (left hand side). The value of A_{ref} is represented by the horizontal dotted line and was set at: (a) 38.0 mm², (b) 30.1 mm², (c) 25.0 mm², (d) 22.5 mm², (e) 20.1 mm², (f) 16.2 mm² and (g) 14.0 mm². The left hand side of this figure shows the solutions of equation (1) for the values of the parameters given in Table 2.

between the onset of the light stimulus and the onset of pupil constriction by using the computer supplied with the Hamamatsu Iriscorder C-2515. The determination of the pupil latency time following light offset is discussed in Results.

RESULTS

Pupil area oscillations

Figure 2 shows pupil area as a function of time for a normal subject (subject A in Tables 1 and 2) when the area threshold, A_{ref}, is set at various levels. When A_{ref} is larger than the initial pupil area, A_i, regular oscillations in pupil area do not occur (Fig. 2a). Repetitive constrictions and dilations in pupil area occur when $A_{ref} < A_i$. The light is turned on ~100 msec after pupil area exceeds A_{ref}. This delay represents the machine delay. The onset of constriction occurs ~300 msec after the light is turned on. This delay is the pupil latency time to light onset. Once pupil area constricts to a value less than

Table 1. Parameters for pupil constriction and dilation measured from single light pulse pupillary responses

Subject	τ^a (msec)	α_c (sec^{-1})	α_d (sec^{-1})	A_{on} (mm^2)	A_{off} (mm^2)
A	380	2.50	0.48	10.0	34.4
B	385	2.50	0.84	15.2	33.6
C	411	3.33	0.50	15.8	34.8
D	400	3.84	0.63	25.2	51.1
E	305[b]	4.87	0.55	14.0	35.5

[a]Total time delay = neural time delay + machine time delay.
[b]Machine time delay was 100 msec for all subjects, except subject E for whom it was 25 msec.

Table 2. Parameters for pupil constriction and dilation from pupil cycling measurements

Subject	τ^a (msec)	α_c (sec^{-1})	α_d (sec^{-1})	A_{on} (mm^2)	A_{off} (mm^2)
A	380	4.46	0.42	11.8	34.0
B	385	3.11	0.74	15.7	34.5
C	411	3.88	0.27	15.5	34.2
D	400	4.69	0.36	26.3	52.4
E	305[b]	5.19	0.46	16.4	39.5

[a]Total time delay = neural time delay + machine time delay.
[b]Machine time delay was 100 msec for all subjects, except subject E for whom it was 25 msec.

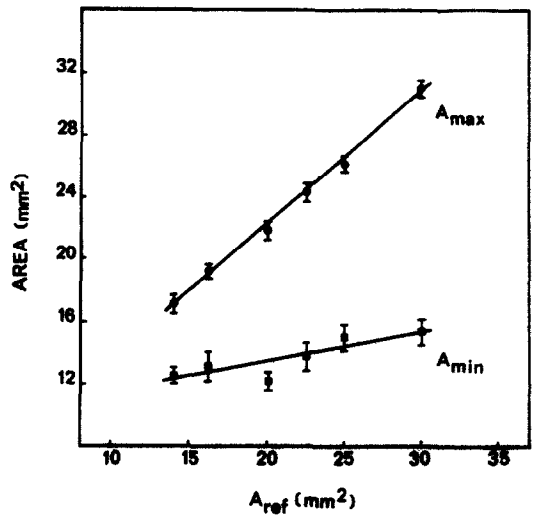

Fig. 3. Plots of A_{max} and A_{min} as a function of the area threshold, A_{ref}, for subject A (Tables 1 and 2 and Fig. 2). Data has been represented as the mean ± 1 SD and is for a range of 12–18 consecutive cycles. Solid lines were determined from a linear regression analysis.

A_{ref}, the light is turned off after the machine delay. The pupil continues to constrict for the duration of another latency (latency time for light offset), after which it begins to dilate. The process repeats and gives rise to cycling.

In the discussion which follows we use the notation τ_c, τ_d to refer to the sum of the machine delay and pupil latency time for, respectively, light onset and light offset.

The period and amplitude of the pupil area oscillations shown in Fig. 2 depend on the choice of A_{ref} relative to A_i. As A_{ref} is brought closer to A_i, the amplitude and period of the pupil area oscillations increase. In addition, the fraction of time that the light is on during each cycle in pupil area decreases ($\sim$0.5 when $A_{ref} = 14.2\,mm^2$ vs 0.1 for $A_{ref} = 30.1\,m^2$). As shown in Fig. 3, the maximum amplitude, A_{max}, and minimum amplitude, A_{min}, of the pupil area oscillations vary linearly as a function of A_{ref}. In contrast, there is a nonlinear relationship between the average period of the pupil area oscillations and A_{ref} (Fig. 4).

First-order model

Background. The pupil light reflex may be viewed as a delayed negative feedback neural control mechanism which regulates the retinal light flux (equal to the light intensity multiplied by the pupil area) by changing the pupil area. The delay arises because of the pupil latency time(s). Pupil cycling occurs when, for example, the gain of the feedback loop is increased (Stark & Cornsweet, 1958; Longtin & Milton, 1989a,b). Self-generated oscillations of this type are referred to as autonomous oscillations. It is important to distinguish autonomous pupil cycling (Fig. 2) from experiments in which oscillations in pupil area occur in response to an independent external light pulse generator ("forced" oscillations) (see, for example, Sun et al., 1983a).

The description of autonomous oscillations in pupil area requires the use of a nonlinear delay–differential equation (Longtin & Milton, 1988, 1989a,b). The nonlinearities arise, for example, because of the logarithmic compression of light intensities at the retina (Weber–Fechner law). For physiologically relevant choices of the feedback function these equations cannot be solved analytically (Longtin & Milton, 1989b). However, under the experimental conditions described in Fig. 1 the feedback function (area comparator) is of a very simple type and the oscillations in pupil area, A, can be described by (Longtin & Milton, 1988, 1989b; Milton, Longtin, Beuter, Mackey & Glass, 1989)

$$\alpha^{-1}\frac{dA}{dt} + A = \begin{cases} A_{on}, & \text{if} \quad A_\tau > A_{ref} \\ A_{off}, & \text{if} \quad A_\tau < A_{ref} \end{cases} \qquad (1)$$

where A_τ is the pupil area at a time τ in the past, i.e. $A_\tau = A(t-\tau)$. Equations of the form of equation (1) are of particular interest for the study of oscillations in feedback mechanisms

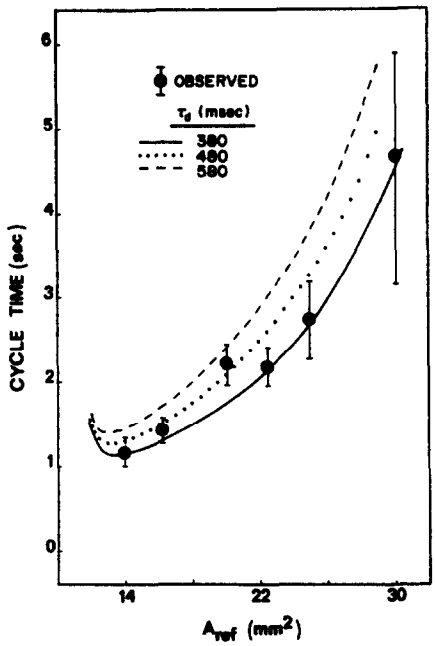

Fig. 4. Comparison of the observed period, T, of pupil cycling as a function of A_{ref} for subject A (Figs 2 and 3) to that predicted by equation (4). Data has been represented as the mean $\pm$ 1 SD and is for a range of 12–18 consecutive cycles. The solid line is the value of T predicted from equation (4) when $\tau_c = \tau_d$. In all calculations, $\tau_c = 380$ msec.

because it is possible to obtain a great deal of mathematical insight into their properties (an der Heiden & Mackey, 1982; Appendix I).

Equation (1) is a first-order model for pupil cycling since both constriction and dilation are described by single exponential processes. However, the rate constant for pupil movements differs for constriction (α_c) and dilation (α_d). Figure 5 shows a typical solution of equation (1). When the light is on, pupil size decreases exponentially to a lower asymptotic area (A_{on}), whereas when the light is off, pupil size increases exponentially towards a higher asymptotic area (A_{off}).

Parameter estimation. In order to compare the first order model for pupil cycling given by equation (1) to the experimental observations in Figs 2–4 it is necessary to estimate seven parameters: α_c, α_d, A_{on}, A_{off}, A_{ref}, τ_c and τ_d. The value of A_{ref} is set by a potentiometer. In our previous study (Longtin & Milton, 1988) we assumed that $\tau_c = t_d$ and estimated the values of α_c, α_d, A_{on} and A_{off} from the changes in pupil area that occur following a 0.5 sec light pulse as shown in Figs 6(a) and (b). The area asymptote, A_{off}, is taken as the initial pupil area and A_{on} is the minimum pupil area following a longer (2 sec) light pulse of the same illuminance. The

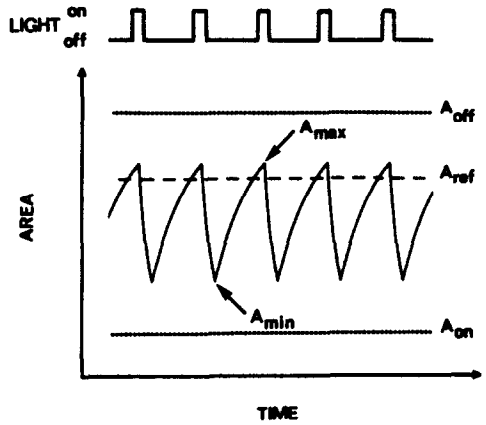

Fig. 5. Detailed representation of a typical solution of equation (1) when $A_{ref} < A_i$. See text for details.

values of α_c, α_d, A_{on} and A_{off} determined in this manner for five normal subjects are listed in Table 1.

Here we show that the parameters α_c, α_d, A_{on} and A_{off} can be estimated directly from pupil cycling measurements. This result follows from the fact that equation (1) can be solved analytically (Appendix I). The solution indicates that a plot of A_{min} vs A_{ref} will be linear (Fig. 3) and specifically that

$$A_{min} = a + bA_{ref} \tag{2}$$

where

$$a = A_{on}(1 - b) \tag{3a}$$

$$b = \exp(-\alpha_c \tau_c). \tag{3b}$$

Since the value of τ_c can be determined experimentally (see Methods), the slope of this plot yields α_c and the intercept A_{on}. An expression equivalent to those given by equations (2) and (3) is found for A_{max} except that α_c, τ_c and A_{on} are replaced, respectively, by α_d, τ_d and A_{off}. Thus the intercept of a plot of A_{max} vs A_{ref} can be used to determine A_{off}. However, since τ_d is not known, the slope of this plot does not permit the value of α_d to be determined uniquely.

Table 2 summarizes the values of α_c, α_d, A_{on} and A_{off} determined from cycling measurements for the same five subjects in Table 1 under the assumption that $\tau_c = \tau_d$. In comparing the results in Tables 1 and 2 it is important to realize that the results in Table 1 are determined from the response to a single light pulse at a single initial pupil area, whereas for cycling these parameters represent, in some sense, an averaging over 50–70 single pulse determinations covering a range of initial pupil areas (i.e. 10 light pulses per area threshold, times 5–7 area

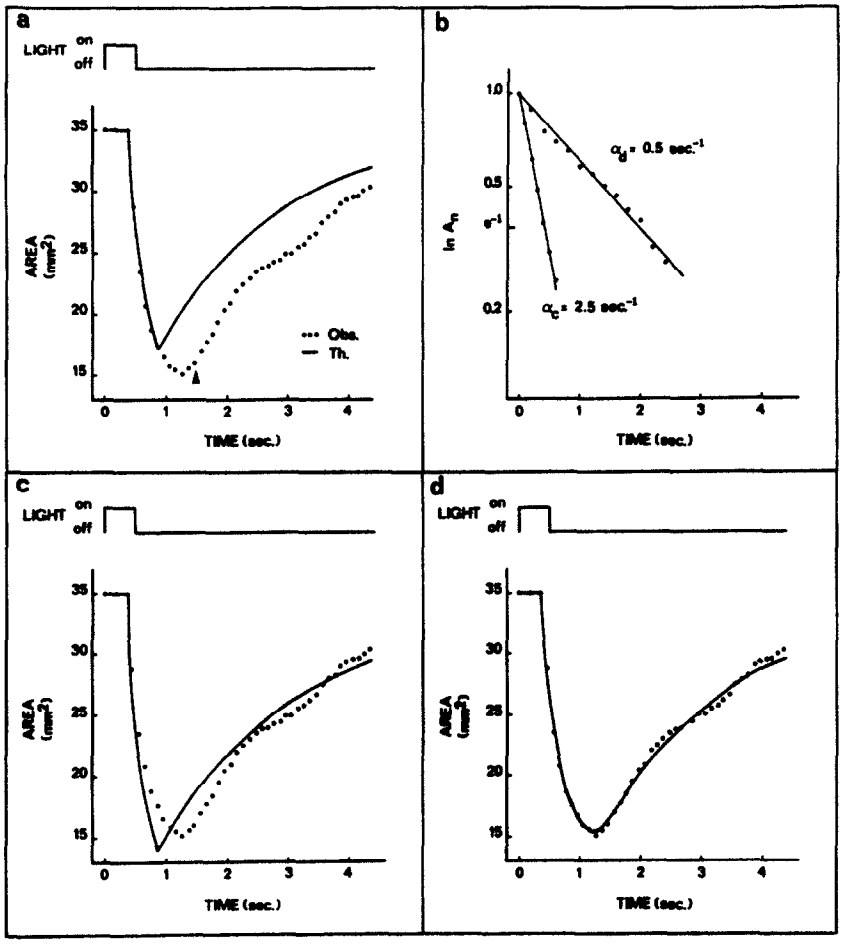

Fig. 6. Pupil area as a function of time, A_t, following a single 0.5 sec light pulse for subject A (dotted line). In (a) the observed pupillary response is compared to that predicted by equation (1) when the parameters are estimated by the single pulse method (solid line, subject A in Table 1, see text for details). The semi-log plots for the determination of α_c, α_d are shown in (b) where A_n is the normalized pupil area, i.e. $A_n = |A_t - A_{on,off}|/|A_i - A_{on,off}|$. For pupil constriction the initial value of A_i was taken as the onset of constriction and for dilation the initial value of A_i was arbitrarily chosen as the point indicated by '▲'. In (c) the observed pupillary response is compared to that predicted by equation (1) when the parameters are estimated from cycling measurements (solid line, subject A in Table 2). In (d) the observed pupil response is compared to an empirical model in which constriction is described by a single exponential process and dilation by two exponentials [i.e. equation (5)]. Details of the parameter estimation for the predicted solution in (d) are given in Appendix II.

thresholds). The values of A_{on} and A_{off} obtained by the two methods are in good agreement; however, the values of α_c and α_d differ. The differences in α_d cannot simply be attributed to the uncertainty in τ_d since an increase in τ_d would decrease the value of α_d even further [equation (3b)].

Figures 6(a) and (c) compare the changes in pupil area that occur following a 0.5 sec light pulse to those predicted from equation (1) when the parameters α_c, α_d, A_{on} and A_{off} have been estimated, respectively, from single pulse measurements (Fig. 6b, Table 1) and pupil cycling measurements (Fig. 3, Table 2). Pupil cycling measurements yield parameters which provide a better description of the pupillary time course when $\tau_c = \tau_d$. Similar results were obtained for all subjects studied. In the discussion which follows we consider only those solutions of equation (1) in which the parameters have been estimated from cycling measurements.

Period of pupil area oscillations. The period of pupil cycling, T, predicted by equation (4) is (Appendix I)

$$T = \tau_c + \tau_d + \alpha_c^{-1} \ln\left[\frac{A_{max} - A_{on}}{A_{ref} - A_{on}}\right] + \alpha_d^{-1} \ln\left[\frac{A_{min} - A_{off}}{A_{ref} - A_{off}}\right]. \quad (4)$$

In Fig. 4 we show the period (T) of pupil cycling (solid line) calculated from equation (4) when $\tau_c = \tau_d$. The agreement between the predicted and observed average period of pupil cycling is typically better than 5–10%.

It should be noted that equation (4) predicts that the period of pupil cycling is not a monotone increasing function of A_{ref}, but passes through a minimum. We were unable to verify this experimentally. With decreases in A_{ref} below 14 mm^2, pupil area would undergo 2–3 cycles with increasing A_{min} until the cycling stopped with the light on and $A_{min} > A_{ref}$. It is not clear whether this phenomena arose because of a type of pupillary escape (Sun & Stark, 1983; Sun, Krenz & Stark, 1983b; Krenz & Stark, 1984) or represents changes in A_{on} due to retinal adaptation (Longtin & Milton, 1988).

Light offset latency time (τ_d). Equation (4) in combination with equations (2) and (3) can also be used to calculate the period (T) of pupil cycling when the latency times for light onset and offset are not the same (i.e. $\tau_c \neq \tau_d$). In Fig. 4 we show the period (T) of pupil cycling calculated from equation (4) for two values of $\tau_d > \tau_c$ [and hence of α_d; see equation (3b)] (dotted lines). As can be seen the best agreement between the predicted and observed periods of pupil cycling occurs when $\tau_c = \tau_d$.

Amplitude of pupil area oscillations. The fact that the values of α_c, α_d, A_{on} and A_{off} are determined from the data in Fig. 3 guarantees that the solutions of equation (1) will have the same average amplitude as observed for pupil cycling (Fig. 2).

Shape of pupil area oscillations. One way to compare the shape of the predicted and observed pupil area oscillations is to plot pupil area as a function of time (Fig. 2). However, the limitations of this method for comparing the shape of oscillations are immediately apparent. The observed pupil area oscillations show small cycle to cycle variations in period and amplitude due to noisy inputs into the pupil light reflex which have not been incorporated into equation (1). Thus one cannot easily compare theory with observation by, for example, superimposing the predicted and observed time series.

A much better method for comparing the shape of predicted oscillations to those observed experimentally involves the construction of a "phase plane diagram". A phase plane diagram is a convenient way of graphing pupil area changes as a function of time since for an oscillation a closed loop trajectory will be obtained. For equation (1) a phase plane diagram can be constructed by plotting $A(t)$ vs $A(t-\tau)$. The advantage of constructing a phase plane diagram is that the overall average shape of the oscillation can be assessed and compared to theory even in the presence of noisy perturbations.

Figure 7 compares the measured phase plane diagrams for different values of A_{ref} to those predicted by equation (1). As plotted the trajectories are traversed in a counter-clockwise direction and the oriented is as follows: the upper right-hand corner corresponds to the change from dilation to constriction and the lower left-hand corner to the change from constriction to dilation. As A_{ref} is changed, the predicted shape of the closed trajectories changes from triangular (Fig. 7a) to roughly quadrilateral (Fig. 7d). Overall there is surprisingly good agreement between the experimentally measured and predicted phase plane trajectories. However, on closer inspection it can be seen that the best agreement between equation (1) and observation occurs for the latter stages of dilation and the earlier stages of constriction.

Alternative models for pupil cycling

The preceding results demonstrate that the period and amplitude of pupil area oscillations can be predicted from a model [equation (1)] in which both constriction and dilation are described by single exponentials and in which the latency times for light onset and offset are the same (Figs 2–4). However, the shape of the predicted oscillations is not exactly the same as that observed (Fig. 7).

We found that a much better fit to the changes in pupil area following a single light pulse was obtained when dilation was represented by a sum of two exponentials (compare Fig. 6d with Figs 6a–c). This fit was obtained with $\tau_c = \tau_d$ (Appendix II). In view of these observations, an alternative model for pupil area oscillations becomes

$$\left.\begin{aligned} \alpha^{-1}\frac{dA}{dt} + A = A_{on} \quad &\text{if} \quad A_\tau > A_{ref} \\ \frac{d^2A}{dt^2} + \delta\frac{dA}{dt} + \omega^2 A = A_{off} \quad &\text{if} \quad A_\tau < A_{ref} \end{aligned}\right\} \quad (5)$$

where δ, ω are constants to be determined. In contrast to the expressions derived from equation (1), it is not possible to obtain simple mathematical expressions for A_{max} and T. Thus

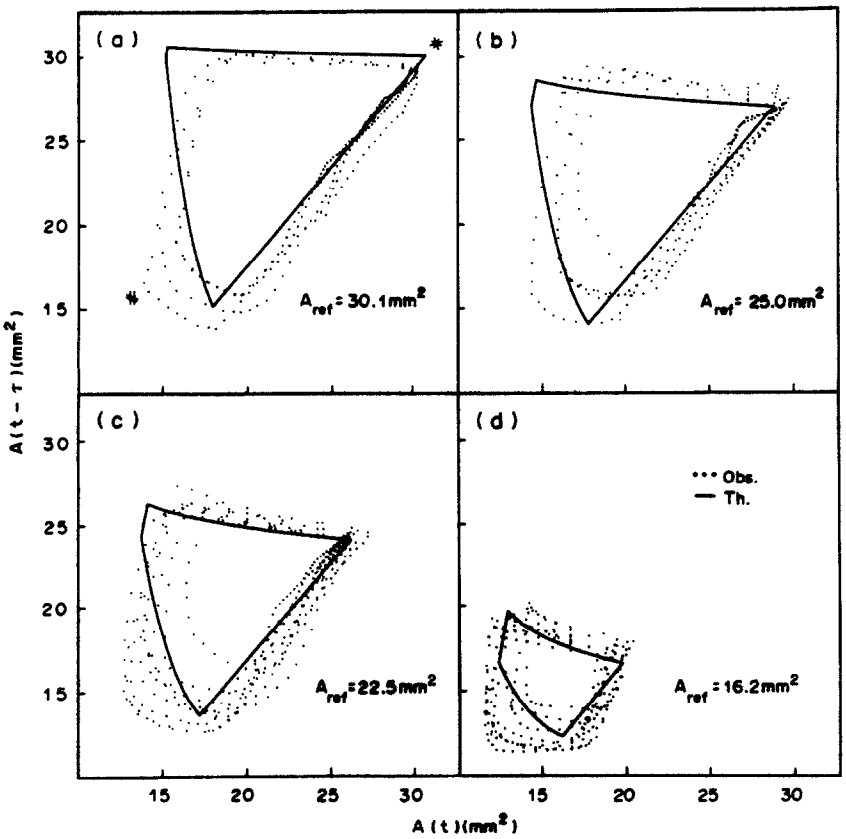

Fig. 7. Phase plane diagrams for pupil cycling as a function of A_{ref} for subject A (Figs 2–4). The data was digitized at a frequency of 20 Hz. Solid lines are those predicted by equation (1) for parameters estimated from the data in Fig. 2 (subject A in Table 2). A_{ref} was set at: (a) 30.1 mm², (b) 25.0 mm², (c) 22.5 mm², and (d) 16.2 mm². The change of constriction to dilation is indicated by # in (a) and the change from dilation to constriction by *.

we cannot presently estimate the three pupillary rate constants and area asymptotes from cycling data in a way more practical than fitting the time course of the pupil area changes following a single light pulse using a nonlinear regression analysis.

Preliminary computer simulations of equation (5) indicate that the shape of the pupil area oscillations closely resemble that of the observed oscillations (data not shown). However, given the difficulties in estimating the required parameters, it is not yet possible to assess the agreement between model and data with certainty.

DISCUSSION

Our observations emphasize the importance of measurements of the amplitude, rather than the period, of pupil area oscillations for obtaining quantitative descriptions of pupillary constriction and dilation. In particular, when pupil area oscillations are produced under conditions of piecewise constant negative feedback (Fig. 1), it is found that the minimum A_{min} and maximum (A_{max}) amplitude vary linearly with A_{ref}. The A_{ref}-dependent changes in A_{min} depend only on factors which influence pupil constriction [see, for example, equation (2)], whereas changes in A_{max} are related only to changes in the factors which influence pupil dilation. This follows from the response assymmetry of the pupil to light onset and offset (Longtin & Milton, 1989a,b). Thus pupil constriction and dilation can be quantitated in terms of the slopes and intercepts of straight line plots. This technique should facilitate the evaluation of efferent pupillary defects.

Quantitative evaluation of pupil responses from measurements of pupil area oscillations produced under conditions of piecewise constant negative feedback offers a number of advantages over measurements following single light pulses and edge-light pupil cycling. By cycling the pupil, the effects of hippus are minimized since high frequency noise is reduced

by the self-filtering action of the resonance peak of the autonomous oscillations which acts as narrow-bandpass filter (Stark, 1962). Second, generating a plot of A_{min} (or A_{max}) vs A_{ref} is in some sense equivalent to averaging 50–70 single light pulses covering a range of initial pupil areas. These measurements are not time consuming: the experiment in Fig. 2 took less than 5 min to complete. Obtaining an averaged pupil response is important in view of the intrinsic variability of the pupil's response to light pulses (Usui & Stark, 1982). Finally, measurements of amplitude show less variability than those of period (compare standard deviations for A_{min}, A_{max} in Fig. 3 to those of period in Fig. 4, especially at the higher values of A_{ref}).

The infrared pupillometer chosen for this type of study must meet two requirements. First, its response time must be sufficiently faster that the pupil responses (20–60 Hz is adequate for most purposes). Second, since the differences between, for example, A_{max} and A_{ref} can be quite small (Fig. 3), it is important that the pupillometer be able to measure pupil area accurately. The 0.01 mm^2 resolution of the pupillometer used in this study appears to be adequate for most purposes. The necessary area comparator (Fig. 1) can be easily installed in both video-type (Ishikawa, Naito & Inabe, 1970; Longtin & Milton, 1988; Milton et al., 1988) and reflectance-type (Stark, 1962; Reulen et al., 1988) pupillometers.

The observation that A_{min} (or A_{max}) varies linearly with A_{ref} can be explained by a mathematical model for pupil cycling [equation (1)] in which both pupil constriction and dilation occur as single exponential processes but with different rate constants. This model also correctly predicts the period of the pupil area oscillations. However, measurements of the period of the oscillations as a function of A_{ref} are not sufficient to identify the individual role of the constricting and dilating mechanisms of the pupil light reflex [equation (4)]. This observation emphasizes the importance of amplitude over period measurements for evaluating the properties of the efferent pathways of the pupil light reflex.

It is generally held that the pupil latency time for light offset (τ_d) is either equal to or longer than the latency time for light onset (τ_c) (see, for example, Löwenstein & Friedman, 1942). However, direct measurement of τ_d is difficult since the onset of dilation following light offset cannot readily be determined by visual inspection. The problem is that pupil area may initially continue to decrease after the onset of dilation because of the effects of the mechanical properties of the iris and its musculature which prevent sudden changes in the sign of the velocity. Thus determination of τ_d from the pupil response to a light pulse requires reference to a mathematical model. On the other hand, it is unlikely that τ_d can be measured directly from the pupil response to a dark pulse. The response of the pupil to either a light or dark pulse is in the same direction ("unidirectional rate sensitivity") (Clynes, 1961). Thus it is unclear whether measurement of a latency to a dark pulse would correspond to the τ_d relevant for pupil cycling measurements. From the standpoint of a first-order model for pupil cycling [equation (1)], the best agreement between the predicted and observed period of the pupil area oscillations occurs when τ_c and τ_d are approximately the same. When the alternative, more complex model for the pupil response to light [equation (5)] was used, the observed pupillary response could also be modelled with $\tau_c = \tau_d$. These observations do not prove conclusively that $\tau_c = \tau_d$, but they are certainly highly suggestive.

The shape of the observed oscillations in pupil area is only approximately described by equation (1). It is possible that by increasing the number of exponentials which describe constriction and/or dilation a better description of the shape of the oscillations can be obtained. In this way insights can be gained into the properties of the efferent properties of the pupil light reflex. For example, we found that a better agreement between the predicted and observed shape of the pupil response to a single light pulse is obtained when dilation is modelled as the sum of two exponentials. The main limitation of this type of approach are the difficulties associated with estimating the required number of parameters from the experimental data.

Our observations do not allow us to identify the neurophysiological mechanisms responsible for pupil dilation during pupil cycling. The role of sympathetic efferents is uncertain given the observations that pupil cycling can be elicited in human subjects even when the sympathetic supply to the pupil is cut surgically (Milton et al., 1988) or blocked pharmacologically (Martyn & Ewing, 1986). A parasympathetic mechanism producing pupil dilation involves active inhibition of the Edinger–Westphal nucleus (Loewenfeld, 1958). Experiments will be re-

quired to determine the relative roles of the sympathetic and parasympathetic mechanisms for producing pupil dilation during pupil cycling.

Studies of the pupil light reflex "clamped" with external electronic feedback have been used previously to determine the influence of the 'linear' and 'nonlinear' properties of the reflex in determining the period and shape of the oscillations (Stark, 1962). Here we have shown that this technique can also be used as a practical method for evaluating the average pupil constriction and dilation. From the more general point of view of the study of oscillations (i.e. nonlinear dynamics), this experimental paradigm of neural control also provides unique opportunities to verify theoretical predictions, to draw attention to unexplained phenomena, and to assess the role of superimposed random variations ("noise") in shaping the observed dynamics (Longtin & Milton, 1988, 1989b; Milton et al., 1989). It can be anticipated that by continuing to exploit this experimental model it will be possible to gain insights into the properties of this reflex by, for example, clever design of the area comparator. Some of these insights may also be applicable to other neural control mechanisms as well.

Acknowledgements—This research was partially supported by the Natural Science and Engineering Research Council of Canada (NSERC) through Grant A-0091. AL was supported by an NSERC post-graduate scholarship. We are grateful to Hamamatsu Photonics Systems, Inc. (Hamamatsu City, Japan and Waltham, MA) for providing the Binocular Iriscorder Model C-2515. We express our gratitude to Dr Trevor Kirkham at the Montreal Neurological Institute for providing laboratory space and encouragement. We thank Drs Michael Mackey, Jacques Bélair, Michael Guevara and Leon Glass and the Neuro-electronics group at the Montreal Neurological Institute for their comments and assistance.

REFERENCES

Clynes, M. (1961). Unidirectional rate sensitivity: A biocybernetic law of reflex and humoral systems as physiological channels of control and communication. *Annals of the New York Academy of Science, 92*, 946–969.

an der Heiden, U. & Mackey, M. C. (1982). The dynamics of production and destruction: Analytic insight into complex dynamics. *Journal of Mathematical Biology, 16*, 75–101.

Ishikawa, S., Naito, M. & Inabe, K. (1970). A new video-pupillography. *Ophthalmologica, 160*, 248–259.

Krenz, W. & Stark, L. (1984). Neuronal population model for the pupil-size effect. *Mathematical Bioscience, 68*, 247–265.

Loewenfeld, I. E. (1958). Mechanisms of reflex dilation of the pupil: Historical review and experimental analysis. *Documenta Ophthalmologica, 12*, 185–448.

Longtin, A. & Milton, J. G. (1988). Complex oscillations in the pupil light reflex with 'mixed' and delayed feedback. *Mathematical Bioscience, 90*, 183–199.

Longtin, A. & Milton, J. G. (1989a). Insight into the transfer function, gain, and oscillation onset for the pupil light reflex using delay-differential equations. *Biological Cybernetics, 61*, 51–58.

Longtin, A. & Milton, J. G. (1989b). Modelling autonomous oscillations in the human pupil light reflex using nonlinear delay-differential equations. *Bulletin of Mathematics and Biology, 51*, 605–624.

Löwenstein, O. & Friedman, E. D. (1942). Pupillographic studies. I. Present state of pupillography; Its method and diagnostic significance. *Archives of Ophthalmology, 27*, 969–993.

Martyn, C. N. & Ewing, D. L. (1986). Pupil cycle time. A simple way of measuring an autonomic reflex. *Journal of Neurology, Neurosurgery and Psychiatry 49*, 771–774.

Miller, S. D. & Thompson, H. S. (1978). Edge-light pupil cycle time. *British Journal of Ophthalmology, 62*, 495–500.

Milton, J. G., Longtin, A., Kirkham, T. H. & Francis, G. S. (1988). Irregular pupil cycling as a characteristic abnormality in patients with demyelinative optic neuropathy. *American Journal of Ophthalmology, 105*, 402–407.

Milton, J. G., Longtin, A., Beuter, A., Mackey, M. C. & Glass, L. (1989). Complex dynamics and bifurcations in neurology. *Journal of Theoretical Biology, 138*, 129–147.

Reulen, J. P. H., Marcus, J. T., van Gilst, M. J., Koops, D., Bos, J. E., Tiesinga, G., de Vries, F. R. & Boshuizen, K. (1988). Stimulation and recording of the dynamic pupillary reflex: The IRIS technique. Part 2. *Medical Biological Engineering Computers, 26*, 27–32.

Semmlow, J. L. & Chen, D. C. (1977). A simulation model of the human pupil light reflex. *Mathematical Bioscience 33*, 5–24.

Stark, L. (1959). Stability, oscillations and noise in the human pupil servomechanism. *Proceedings of IRE 47*, 1925–1939.

Stark, L. (1962). Environmental clamping of biological systems: Pupil servomechanism. *Journal of the Optical Society of America, 52*, 925–930.

Stark, L. & Cornsweet, T. N. (1958). Testing a servoanalytic hypothesis for pupil oscillations. *Science, New York, 127*, 588.

Stark, L. & Sherman, P. M. (1957). A servoanalytic study of consensual pupil reflex to light. *Journal of Neurophysiology, 20*, 925–930.

Stern, H. J. (1944). A simple method for the early diagnosis of abnormality of the pupillary reaction. *British Journal of Ophthalmology, 28*, 275–276.

Sun, F. & Stark, L. (1983). Pupillary escape intensified by large pupillary size. *Vision Research 23*, 611–615.

Sun, F., Tauchi, P. & Stark, L. (1983a). Binocular alternating pulse stimuli: Experimental and modelling studies of the pupil reflex to light. *Mathematical Bioscience 67*, 225–245.

Sun, F., Krenz, W. C. & Stark, L. (1983b). A systems model for the pupil size effect. I. Transient data. *Biological Cybernetics 48*, 101–108.

Ukai, K., Higashi, J. T. & Ishikawa, S. (1980). Edge-light pupil oscillation of optic neuritis. *Neuroophthalmology, 1*, 33–43.

Usui, S. & Stark, L. (1982). A model for nonlinear stochastic behaviour of the pupil. *Biological Cybernetics 45*, 13–22.

APPENDIX I

Solution of Equation (1)

The oscillations in pupil area produced by equation (1) (Fig. 5) are referred to as limit cycles. Assume that the motion described by equation (1) has settled onto the limit cycle oscillation. Then we can write the solution as

$$A(t) = \begin{cases} A_{on} + [A(t_0) - A_{on}][\exp(-\alpha_c(t - t_0))], \\ \quad \text{if} \quad A(s - \tau) > A_{ref} \\ A_{off} + [A(t_0) - A_{off}][\exp(-\alpha_d(t - t_0))], \\ \quad \text{if} \quad A(s - \tau) \leqslant A_{ref} \end{cases} \tag{A1}$$

where $s \in (t_0, t)$. Let A_{max} (A_{min}) denote the maximal (minimal) area reached by the oscillations (Fig. 5). Then

$$A_{ref} = A_{max} \exp(-\alpha_c t_1) + A_{on}[1 - \exp(-\alpha_c t_1)] \tag{A2a}$$

$$A_{ref} = A_{min} \exp(-\alpha_d t_2) + A_{off}[1 - \exp(-\alpha_d t_2)] \tag{A2b}$$

from which we can easily obtain

$$t_1 = \alpha_c^{-1} \ln\left[\frac{A_{max} - A_{on}}{A_{ref} - A_{on}}\right] \tag{A3a}$$

$$t_2 = \alpha_d^{-1} \ln\left[\frac{A_{min} - A_{off}}{A_{ref} - A_{off}}\right] \tag{A3b}$$

The period, T, is equal to $\tau_c + \tau_d + t_1 + t_2$. The values of A_{min} *and* A_{max} (equations (2) and (3) in text) can be determined from equation (A1) by choosing $A(t_0) = A_{ref}$.

It was found both analytically and numerically that these limit cycle solutions of equation (1) are very stable. In fact, the transients leading to the limit cycle behaviour decay very quickly.

APPENDIX II

Parameter Estimation for Equation (5)

In order to fit equation (5) to the response of the pupil to a single light pulse (Fig. 6) we imposed four constraints: (1) the transition from constriction to dilation occurs at time $t_c + T_p$ where t_c is the time of constriction onset ($\sim$300 msec after light pulse falls on retina) and T_p is the light pulse duration (500 msec); (2) the pupil area is continuous at time $t = T_p$; (3) the area velocity is continuous at time $t = T_p$; and (4) the initial pupil area is fixed.

If we let $t_c = 0$ and denote pupil area by $A(t)$, we have:

$$A(t) = \begin{cases} A_c(t) = A(0) + B[\exp(-\alpha_c t) - 1], \\ \quad \text{if} \quad 0 < t < T_p \\ A_d(t) = C \exp[-\mu_d(t - T_p)] \\ \quad + D \exp[-\beta_d(t - T_p)] + E, \\ \quad \text{if} \quad t > T_p \end{cases} \tag{A4}$$

where δ in equation (5) corresponds to $-\mu_d - \beta_d$ and ω^2 to $\mu_d\beta_d$. The constraints (2) and (3) are used to express parameters D and E as a function of the parameter set to be determined by nonlinear regression: $\{B, C, \alpha_c, \mu_d, \beta_d\}$. For the data in Fig. 6 our fit produces $A = 21.81\ \text{mm}^2$, $C = 10.14\ \text{mm}^2$, $\alpha_c = 3.44\ \text{sec}^{-1}$, $\alpha_d = 2.83\ \text{sec}^{-1}$ and $\beta_d = 0.58\ \text{sec}^{-1}$ with a χ^2 value of 10.62 ± 0.54. The value of β_d corresponds to α_d in equation (1). Note that α_d and α_c have not changed significantly from those determined for the first order model (Tables 1 and 2).